

Capacity Fading Mechanism in All Solid-State Lithium Polymer Secondary Batteries Using PEG-Borate/Aluminate Ester as Plasticizer for Polymer Electrolytes

By Fuminari Kaneko, Shinta Wada, Masanobu Nakayama,*
Masataka Wakihara, Jun Koki, and Shigeeki Kuroki

Solid-state lithium polymer secondary batteries (LPB) are fabricated with a two-electrode-type cell construction of Li|solid-state polymer electrolyte (SPE)|LiFePO₄. Plasticizers of poly(ethylene glycol) (PEG)-borate ester (B-PEG) or PEG-aluminate ester (Al-PEG) are added into lithium-conducting SPEs in order to enhance their ionic conductivity, and lithium bis-trifluoromethanesulfonimide (LiTFSI) is used as the lithium salt. An improvement of the electrochemical properties is observed upon addition of the plasticizers at an operation temperature of 60 °C. However, a decrease of discharge capacities abruptly follows after tens of stable cycles. To understand the origin of the capacity fading, electrochemical impedance techniques, ex-situ NMR and scanning electron microscopy (SEM)/energy dispersive X-ray spectroscopy (EDS) techniques are adopted. Alternating current (AC) impedance measurements indicate that the decrease of capacity retention in the LPB is related to a severe increase of the interfacial resistance between the SPE and cathode. In addition, the bulk resistance of the SPE film is observed to accompany the capacity decay. Ex situ NMR studies combined with AC impedance measurements reveal a decrease of Li salt concentration in the SPE film after cycling. Ex situ SEM/EDS observations show an increase of concentration of anions on the electrode surface after cycling. Accordingly, the anions may decompose on the cathode surface, which leads to a reduction of the cycle life of the LPB. The present study suggests that a choice of Li salt and an increase of transference number is crucial for the realization of lithium polymer batteries.

1. Introduction

The rechargeable lithium ion battery is a device that meets crucial demands of our modern society, such as acting as the power source of various portable devices, and in the future is expected to be implemented for large-scale use, for example, in electric vehicles, as energy storage systems for day-to-night power shifts, and so on. However, conventional lithium ion batteries suffer from safety problems because of the volatile and flammable organic solvents in the electrolyte solution. Therefore, alternative materials for the electrolyte are urgently needed today. In this respect, an all-solid-state lithium polymer battery (LPB) that uses lithium conducting solid-state polymer electrolytes (SPEs) has been recognized as one of the most attractive technologies, since they are safer and have a higher energy density upon formation in comparison with conventional batteries that use organic solvents.^[1,2]

Poly(ethylene oxide) (PEO) and its derivatives have been known as a typical representative of a polymer matrix for SPE since the studies by Wright et al. and Armand et al. on their lithium conductivity.^[2,3]

However, PEO-based SPEs show a relatively low ionic conductivity (approx. 10^{-7} to 10^{-5} S cm⁻¹) at room temperature.^[4] To improve this, we have prepared tris(methoxy poly(ethylene glycol)) borate ester (B-PEG)^[5-8] and tris(methoxy poly(ethylene glycol)) aluminate ester (Al-PEG)^[9] as new plasticizers, and the ionic conductivity has been successfully increased by adding B-PEG or Al-PEG into PEO-based polymer electrolytes. For example, the ionic conductivity for B-PEG (or Al-PEG) added to a PEO-based SPE showed more than 10^{-4} S cm⁻¹ at room temperature, while that of SPE without these plasticizers was around 10^{-5} S cm⁻¹. In addition, group 13 elements in B-PEG and Al-PEG may possess Lewis acidity, so that anions of lithium salts would be attracted to B-PEG/Al-PEG plasticizers. Therefore, it is expected that these plasticizers enhance the dissociation of lithium salts and the transport numbers of Li ions, as well as improve the ionic conductivity.^[10]

[*] Prof. M. Nakayama, F. Kaneko, S. Wada, Prof. M. Wakihara
Department of Applied Chemistry
Graduate School of Science and Engineering
Tokyo Institute of Technology
2-12-1 Ookayama Meguro-ku Tokyo 152-8552 (Japan)
E-mail: masanobu@apc.titech.ac.jp

J. Koki
Central for Advanced Materials Analysis
Tokyo Institute of Technology
2-12-1 Ookayama Meguro-ku Tokyo 152-8552 (Japan)
Prof. S. Kuroki
Department of Chemistry and Materials Science
Graduate School of Science and Engineering
Tokyo Institute of Technology
2-12-1 Ookayama Meguro-ku Tokyo 152-8552 (Japan)

DOI: 10.1002/adfm.200800789

Using the above SPEs, an LPB has been fabricated with a cell construction of $\text{Li}|\text{SPE}|(\text{LiCoO}_2 \text{ or } \text{LiFePO}_4)$ and their electrochemical behavior has been studied.^[11] Although the addition of B-PEG improved the rate performance of the LPB, an enhancement of cyclability was not indicated. Therefore, improvement of the ionic conductivity of SPEs is not sufficient to realize stable cycling in an LPB. The alternating current (AC) impedance measurements of the cell indicated that an increase in the interfacial resistance of the SPE|cathode might play an important role in the decay of cycle performance.

In this work, LPBs have been fabricated using B-PEG or Al-PEG plasticizers, and AC impedance spectroscopy, pulsed field-gradient stimulated-echo sequence (PGStE)-NMR spectroscopy, and scanning electron microscopy (SEM)/energy dispersive X-ray spectroscopy (EDS) techniques are performed in order to reveal the capacity fading mechanism.

2. Results and Discussion

2.1. Electrochemical Performance

Figure 1a presents the variation of the capacity retention with cycle numbers for an all solid-state LPB without plasticizer in the SPE film. The corresponding charge–discharge curves for selected cycle numbers are also presented in Figure 2a. Typical flat-shaped voltage profiles are observed around 3.4–3.5 V, which indicates that a two phase coexistence reaction proceeded in an olivine-type LiFePO_4 cathode as reported previously.^[12] After the initial five cycles, the LPBs showed a capacity higher than 120 mA h g^{-1} . However, a severe decrease of capacity retention followed after ~ 10 cycles, and the capacity reached almost zero

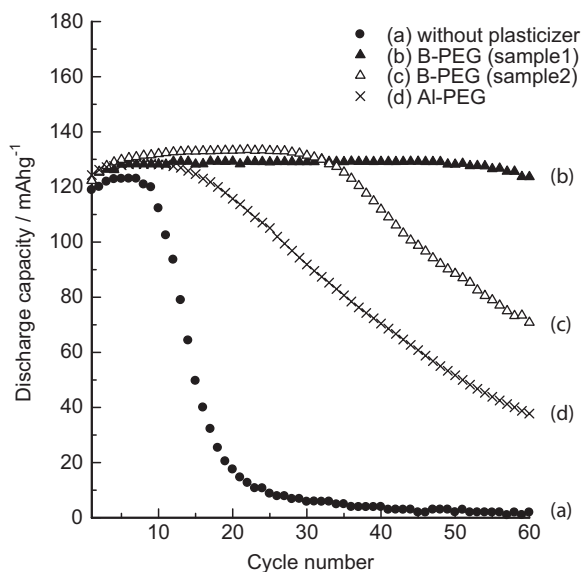


Figure 1. Cycle performance for the LPBs with or without plasticizers of B-PEG or Al-PEG. The charge–discharge tests were performed at 60°C under a current density of 1.0°C ($\sim 200 \mu\text{m}$). Two different results for LPBs using B-PEG with the same cell construction are shown in (b) and (c) as sample 1 and 2, respectively. The details are given in the text.

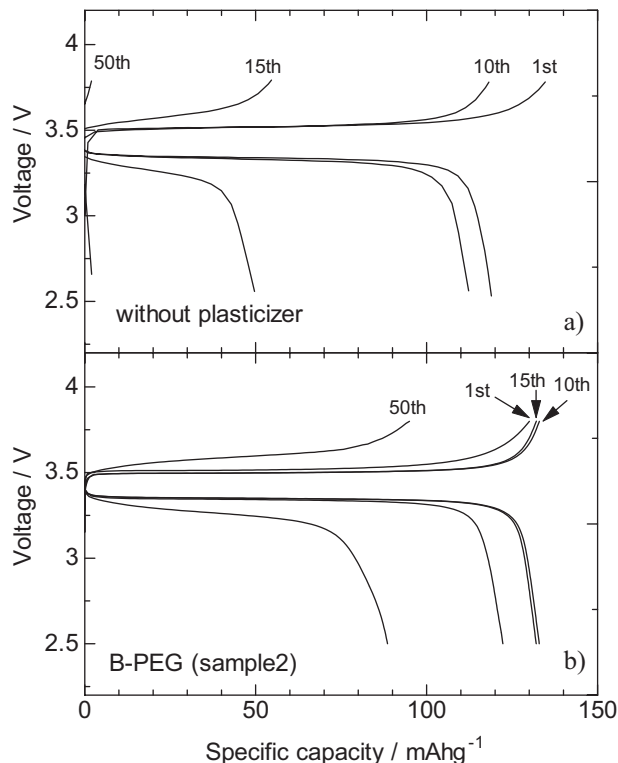


Figure 2. Charge–discharge profiles of a) LPB without plasticizers and b) with B-PEG plasticizer (sample 2). The data correspond to that presented in Figure 1.

after 20 cycles. One of the conceivable reasons for the poor cyclability is a low ionic conductivity of the SPE film. Nevertheless, a sufficiently large discharge capacity ($>120 \text{ mA h g}^{-1}$) at the first cycle indicated that a poor ionic conductivity is not a dominant contribution to the severe decay of capacity retention after ~ 10 cycles at an elevated temperature of 60°C . In fact, the ionic conductivity value of SPE without plasticizer was around $\sim 10^{-4} \text{ S cm}^{-1}$ at 60°C ,^[9] which indicates that the estimated polarization that arises from the SPE bulk resistance would be $\sim 0.03 \text{ V}$ for our LPB construction. Hence, a poor ionic conductivity of the SPE may not explain the abrupt decay phenomena after 10 cycles. (Note, however, that the poor ionic conductivity of the SPE without plasticizers is crucial to the cell performance at room temperature. In our previous study,^[11] almost no capacity was observed for the SPE without plasticizer at 40°C , while the LPB cycled with a capacity of $\sim 80 \text{ mA h g}^{-1}$ upon addition of B-PEG.) On the other hand, an abrupt increase in polarization with a decrease of capacity retention at around 10–20 cycles is observed in the charge–discharge profiles, such that the capacity decay is a result of the polarization other than the ionic conductivity contribution.

Figure 1b–d shows the variation of the capacity retention up to 60 cycles for LPBs with B-PEG and Al-PEG plasticizers. One can see obvious improvements of cycle performance upon using plasticizer. Even though the LPBs shown in Figure 1c and d show a reduction of capacity retention after tens cycles, these LPBs did not fall to zero in capacity as observed for the LPB without plasticizer (Fig. 1a). Such phenomena could be reproduced for all

the LPBs in this study. Therefore, it is expected that the addition of plasticizers suppress the so-called sudden death of LPB during cycling.

In detail, an SPE film to which plasticizers has been added shows a stable capacity retention during the initial tens of charge–discharge cycles. However, after stable cycling, the cell capacity is reduced gradually. For example, B-PEG-added LPB (sample 2, Fig. 1c) shows stable cycling for up to 40 cycles, followed by a gradual capacity decrease. Note that the number of stable cycles is not perfectly reproducible despite the same cell construction. For instance, although the cell construction and materials used in the LPB are the same between sample 1 and 2 where B-PEG plasticizer is added, the cycle performance for both cells is different, as shown in Figure 1b and c. Such a tendency is also observed for the LPBs using Al-PEG plasticizers. One of the conceivable reasons for this is that the phenomena is triggered by undesirable side reactions at the electrode|electrolyte interfacial region, and this reaction product blocks ion exchange at the interface and/or enhances the decay of the bulk SPEs. In fact, the polarization of the charge–discharge reaction increased as the cell capacity reduced. Figure 2b presents voltage profiles for selected cycle numbers for LPB using B-PEG (sample 2). During the stable capacity region, no marked increase of polarization is observed (1st to 15th cycle), while a large polarization is indicated in the voltage profile at the 50th cycle. Therefore, it is expected that an increase in the internal resistance of the LPB would correspond to the fading capacity of the cell.

In order to clarify the details of polarization with respect to the cycle performance, the AC impedance evolution of the LPB with B-PEG (sample 2) and Al-PEG plasticizers has been investigated. Figures 3 and 4 show Nyquist plots of the experimental impedance spectra (cross symbols) for the LPBs using B-PEG (Fig. 3) and Al-PEG (Fig. 4) at the 1st and 60th cycles. Nyquist plots for LPB using B-PEG plasticizer (Fig. 3) consist of two semicircles in a higher frequency region, and a straight line at around 45° against the real part of the impedance (Z') axis in a lower frequency region. According to the literature, the two semicircles correspond to a charge-transfer reaction at the Li-metal|SPE interface (higher frequency side) and SPE|cathode interface (lower frequency side), respectively.^[13] Figure 3c shows Nyquist plots for a Li|SPE|Li symmetric cell using SPE with B-PEG where no SPE|cathode interfacial resistance is expected to appear. The Nyquist plots consist of one semicircle whose frequency range agrees with the semicircle at a higher frequency shown in Figure 3a and b. Hence, the semicircle for the higher frequency region can be assigned to the Li|SPE interface, and that at the lower frequency is the SPE|cathode interface. The straight line that appears at the lowest frequency regime is a resistance attributable to the diffusion driven concentration gradient around the SPE|cathode interface. The intersection of the impedance spectra of the highest frequency region against the Z' axis corresponds to the bulk resistance of the SPE film. Moreover, an additional semicircle is observed at a higher frequency region centered around 20 000 Hz in LPBs that use Al-PEG plasticizer (Fig. 4). This semicircle may represent the resistance of the surface film on the electrode, or a solid electrolyte interface (SEI) that is often observed in lithium ion batteries.^[14–16] As such, the two semicircles can be assigned to the Li|SPE (higher frequency side) and SPE|cathode (lower frequency side) interface resis-

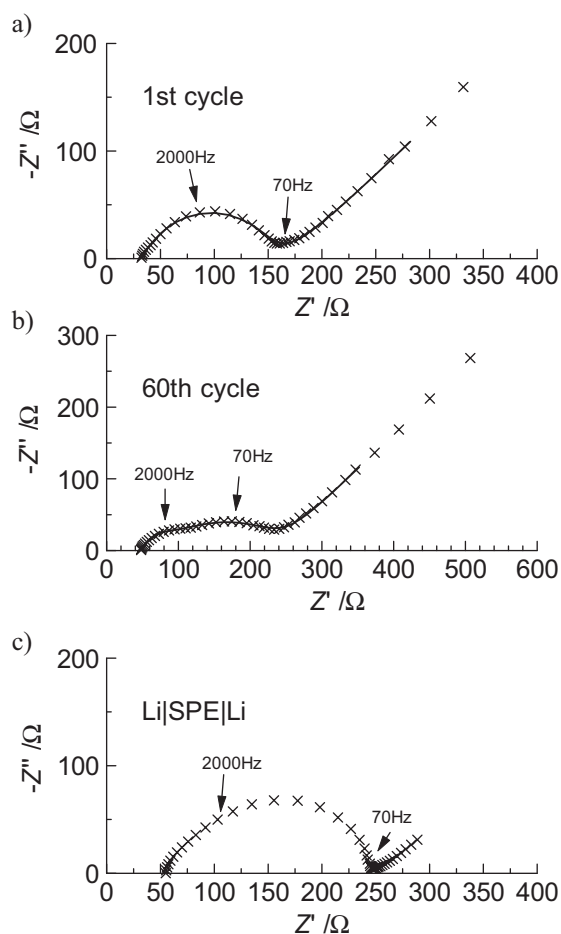


Figure 3. Typical Nyquist plots of AC impedance spectra (cross symbols) for LPB using B-PEG plasticizers (sample 2) at the a) 1st and b) 60th cycles. The corresponding cycle performance data are shown in Figure 1c. The fitted curves are also shown by a hatched line using an equivalent circuit presented in Figure 5a. c) Nyquist plot of a Li|SPE|Li symmetric cell using an SPE film with B-PEG plasticizer.

tances, respectively, by comparing Nyquist plots for the Li|SPE|Li cell shown in Figure 3c. To perform a quantitative analysis, the impedance spectra were curve fitted by using the equivalent circuit shown in Figure 5, which is a modified circuit proposed in previous literature.^[17] In Figure 5, R_1 , R_{SEI} , R_2 , and R_3 represent the resistance as a result of ionic conduction in the bulk of SPE, resistance of SEI, charge transfer at the Li metal|SPE interface and at the SPE|cathode interface, respectively. The C_{SEI} is the capacitance for SEI, and the CPE_1 and CPE_2 are constant phase elements, denoted by $Z_{CPE}^* = A(j\omega)^{-\alpha}$, which was replaced with capacitance by taking into account the distribution of the relaxation time or the non-uniform distribution of current because of the rough nature of the electrode. To fit the lowest frequency region, we added the infinite length Warburg (ILW) impedance, which is described as $Z_{ILW}^* = Z_R(j\omega)^{-0.5}$. Details about the impedance components used in the present equivalent circuit model are described in Ref. [18]. Note that the resistor–capacitor (RC) parallel circuit for SEI impedance was eliminated for the LPB using B-PEG because of a negligible contribution in

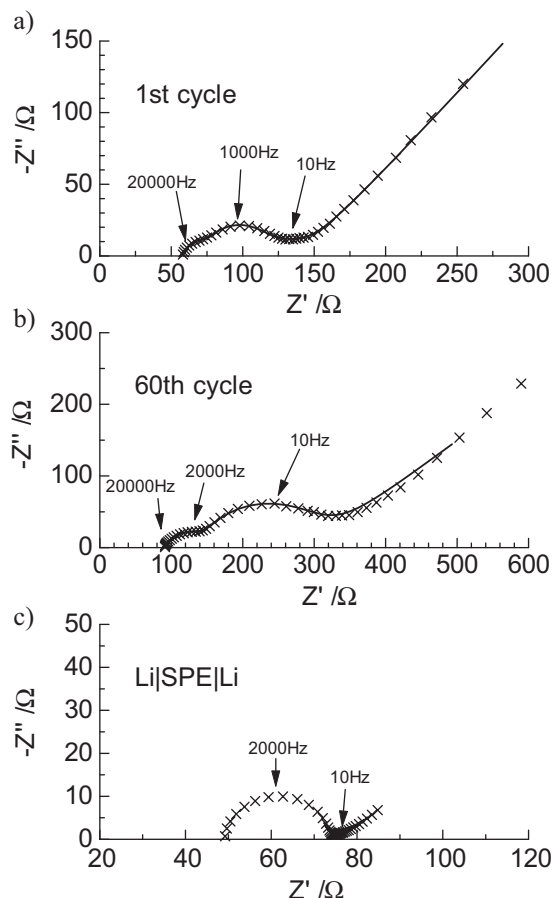


Figure 4. Typical Nyquist plots of AC impedance spectra (cross symbol) for LPB using Al-PEG plasticizers at the a) 1st and b) 60th cycles. The corresponding cycle performance data are shown in Figure 1d. The fitted curves are also shown by a hatched line using an equivalent circuit presented in Figure 5b. c) Nyquist plot of a Li|SPE|Li symmetric cell using an SPE film with Al-PEG plasticizer.

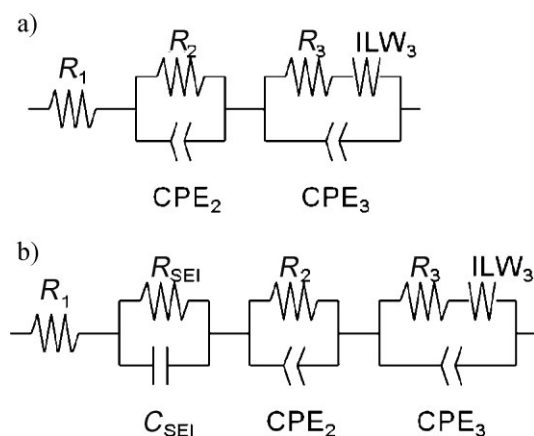


Figure 5. Equivalent circuit for the curve fittings of impedance spectra. Circuits (a) and (b) were used for LPBs using B-PEG and Al-PEG plasticizers, respectively. R_i , C_i , CPE_i , and ILW_i indicate resistance, capacitance, constant phase elements, and infinite length Warburg impedance of component i , respectively. Their mathematical notation and details are given in the text.

the impedance spectra. Typical results of curve fittings are presented in Figures 3 and 4, and show a good agreement of the experimental (cross symbol) with the calculated impedance spectra (solid line). The goodness of fit, χ^2 , is less than the order of 10^{-4} for all the fitting procedures. The best results of the fitted resistances R_1 , R_2 , R_3 , and R_{SEI} , are summarized in Figures 6 and 7 as a function of cycle number for the LPB using B-PEG (Fig. 6) and Al-PEG plasticizers (Fig. 7), respectively. (Note that the impedance data in Figs 6 and 7 correspond to the results shown in Fig. 1c and d, respectively.) In the case of the LPB using B-PEG plasticizer, stable capacity retention continued during an initial 30 cycles, and R_1 and R_2 remained constant. A small gradual increase of R_3 was observed in this regime. The capacity retention then began to decrease gradually after stable cycling up to the 30th cycle. Meanwhile, the R_3 showed a discontinuous increase, so that the decrease of the capacity retention corresponded to the deterioration of the SPE|cathode interface. It is noted that the bulk resistance of R_1 also showed a gradual increase after the 30th cycle without a discontinuous rise as in the case of R_3 . On the other hand, the resistance of R_2 began to decrease gradually from the ~ 30 th cycle. A similar tendency is also observed in the case of the LPB using Al-PEG plasticizers, in which the cell capacity began to decrease after stable cycling up to the ~ 15 th cycle. The increase of resistance was indicated for R_1 and R_3 , which corresponds to the decrease of capacity retention. In detail, the increase of R_3 was remarkable and started around the 10th cycle, being earlier than the decrease of capacity retention in LPB. On the other hand, the increase of R_1 started simultaneously with the decrease of capacity retention. R_2 was almost constant except for the fluctuation around the initial 10 cycles. The same tendency as the behavior of R_2 was observed in R_{SEI} , which did not appear in the LPB using B-PEG plasticizers. Since R_{SEI} remained almost constant up to 60 cycles, stable film formation may be indicated at the surface of the anode and/or cathode electrodes.

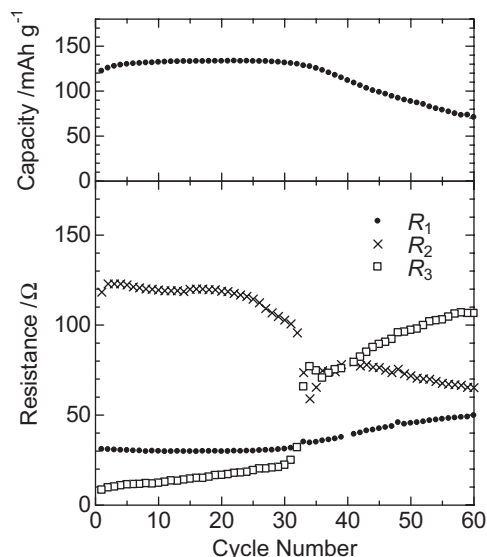


Figure 6. Variation of each resistance versus cycle number of the LPB using B-PEG plasticizer. R_1 , R_2 , and R_3 correspond to the resistances due to bulk of SPE, Li|SPE interface and SPE|cathode interface, respectively.

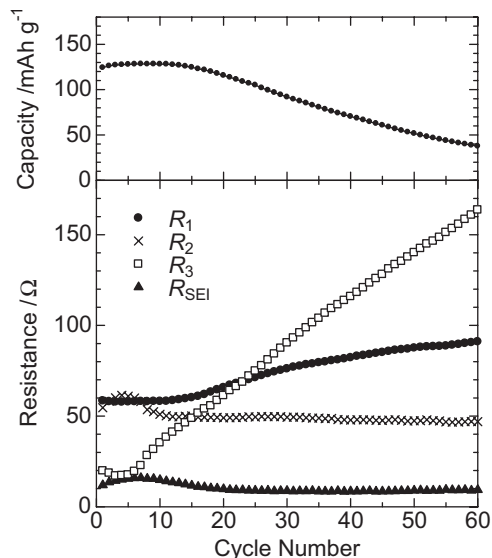


Figure 7. Variation of each resistance versus cycle number of the LPB using Al-PEG plasticizer. R_1 , R_2 , R_3 , and R_{SEI} correspond to the resistances attributable to bulk SPE, the Li|SPE interface, the SPE|cathode interface, and SEI, respectively.

The details of the impedance evolution with respect to the cycle performance are different between the LPBs using B-PEG and Al-PEG plasticizers. However, the key factors that relate to the capacity decay would be an increase of R_1 and R_3 , or deterioration of the bulk and SPE|cathode interface for both the LPBs. In particular, a gradual increase of R_3 in advance of the capacity decay may indicate a continuous accumulation of undesirable side-reaction products on the surface of the LiFePO_4 .

We assume two scenarios such that: i) accumulation of a side reaction product and/or ii) deterioration of the bulk conductivity are directly responsible for the capacity decay. The first assumption is that the side reaction is irreversible, and the products corrupt the bulk conductivity and capacity retention after reaching a critical amount by accumulation. Moreover, the accumulation of side-reaction product would finally reach a percolation limit for ion exchange paths between LiFePO_4 and SPE in the composite cathode matrix. On the other hand, the second assumption is that lithium ion conduction is almost hindered in the bulk of the SPE film. However, the increase in bulk resistance of the SPE film is relatively smaller than the resistance of the SPE|cathode interface as shown in Figures 6 and 7. Hence, a potential explanation for the second assumption is that the AC impedance solely detects the anion conduction part, since the AC impedance method cannot distinguish between the lithium ion and anion conductivity in the bulk. That is to say, the second assumption considers that the transportation number of Li is severely lowered in the bulk of SPE.

2.2. Ex Situ Studies by PGStE-NMR Spectroscopy

As suggested above, we assumed the decrease of transportation number in the SPE bulk was related to the decrease of capacity retention. To clarify the change in SPE, PGStE-NMR measure-

ments were performed using SPE samples before and after charge–discharge cycles. In this study, thicker SPE films (~ 1 mm) that contained the B-PEG plasticizer were used and cycled 60 times at a slower rate at 0.5 C. The total ionic conductivity of the SPE bulk was checked by the AC impedance technique^[10] before fabrication of the LPB, and the bulk resistance was monitored during cycling as shown in Figure 6. A similar cycle performance was obtained as shown in Figure 1c. The diffusion coefficient of the Li and F nuclei, D_{Li} and D_{F} , were estimated from the diffusion attenuation of the spin-echo using the equation:

$$A(g^2) = A(0) \exp[-\gamma^2 \delta^2 g^2 D(\Delta - \delta/3)]. \quad (1)$$

Details of Equation (1) are described elsewhere.^[19] Since fluorine atoms were only contained in the Li salt, lithium bis(trifluoromethanesulfonyl)imide ($\text{LiN}(\text{CH}_3\text{SO}_2)_2$ (LiTFSI), in the LPB, the diffusion coefficient D_{F} simultaneously represents the diffusion coefficient of the anion part of LiTFSI. In addition, since the dissociation ratio of LiTFSI in SPE with B-PGE plasticizers is almost unity,^[10] the transportation number of Li, t_{Li} , was calculated by using the equation:

$$t_{\text{Li}} = D_{\text{Li}} / (D_{\text{Li}} + D_{\text{F}}) \quad (2)$$

along with previous reports.^[20,21] Table 1 lists the obtained ionic conductivities, diffusion coefficients, and transportation number before and after 60 cycles. The ionic conductivity measured by the AC impedance method showed an obvious drop (about 56% with respect to initial conductivity). On the other hand, both of the diffusion coefficients, D_{Li} and D_{F} , and transportation number of Li, t_{Li} , remained constant before and after cycling. Hence, the second scenario that assumes a severe drop of t_{Li} was ruled out. In addition, no changes in D_{Li} and D_{F} suggested that the ionic conduction mechanism inside the SPE bulk was maintained before and after cycling. Therefore, the PGStE-NMR study combined with AC impedance measurements revealed that the increase in bulk resistance stemmed from a decrease of Li salt concentration. It is possible that the Li salt was consumed by a side-reaction that occurred at the SPE|cathode interface as suggested in the previous section.

2.3. Ex-situ studies by SEM/EDS

Figure 8a presents an SEM image of the cross section of the SPE|cathode interface of LPB after 50 cycles, in which the cell capacity decreased to 30% with respect to the fresh cell capacity.

Table 1. Comparison of bulk resistance (R_1), diffusion coefficients of Li (D_{Li}) and F (D_{F}), transference number of Li (t_{Li}) before cycling and after 60 cycles of the LPB using B-PEG plasticizers. All the measurements were performed at 60 °C.

Methods	Impedance		PGSTE-NMR	
	R_1 [Ω]	D_{Li} [$\text{cm}^2 \text{s}^{-1}$]	D_{F} [$\text{cm}^2 \text{s}^{-1}$]	t_{Li}
Before cycle	100	9.00×10^{-8}	1.73×10^{-7}	0.342
After 60 cycles	174	8.33×10^{-8}	1.83×10^{-7}	0.313

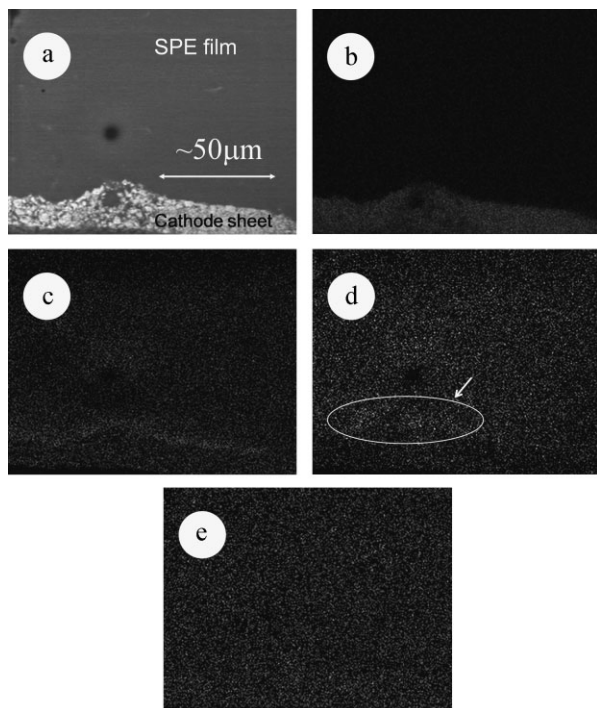


Figure 8. a) SEM image of the cross section of the SPE|cathode interface. Elemental distribution of b) Fe, F, c) Al, and d) Al, and e) Cl corresponding to SEM images by EDS analysis.

As seen in Figure 8a, good contact was maintained between the cathode and SPE film, so that the peeling of the SPE film is a reason for the decrease of capacity. Figure 8b–e shows the elemental distribution of Fe, F, Al, and Cl, respectively, obtained by EDS analysis for the cross section of the SPE|cathode interface. Obviously, iron is resident in the ceramic particles of LiFePO_4 after cycling. Hence, metal dissolution was unlikely to be occurring in the SPE at the EDS analysis level, which was reported for the conventional battery system with a LiMn_2O_4 cathode and a liquid electrolyte at elevated temperature.^[22] On the other hand, the fluorine, chlorine, and aluminum distribution may represent the distribution of TFSI anions, ClO_4^- anions, and Al-PEG plasticizer, respectively. As mentioned later in the experimental section, LiTFSI and Al-PEG are initially distributed only in the SPE film, while LiClO_4 is distributed only in the composite cathode sheets as binder polymer. However, all of these salts and plasticizers disperse into both areas of the SPE film and cathode sheet. Hence, a smooth mass transportation of ions and plasticizers between the SPE and cathode areas is indicated by the EDS analysis. One can see an area concentrated in fluorine at the SPE|cathode interface region after 50 cycles. The reasons are yet undetermined, but it is expected that TFSI reacts with the cathode materials to form undesirable by-products that contain fluorine atoms. A similar tendency has also been observed for the Al distribution (see arrow in Fig. 8d), but the degree of Al concentration in this experiment was within experimental error. Further study is needed to clarify the Al-PEG distribution. Since the Al-PEG may interact with TFSI anions because of its Lewis acidity,^[10] it would be expected that the Al-PEG was involved in side reactions, such as the decomposition of TFSI anions on the

cathode sheet. Such a side reaction would relate to the cell capacity fading as observed in Figure 1. The second scenario as mentioned Section 2.1 is that the by-products (F concentrated region) interrupt the lithium ion exchange between the cathode and SPE film. After reaching a critical amount (or percolation limit) of by-products, the paths for lithium ion exchange might be blocked, which causes a severe decay of capacity as seen in Figure 1. The occurrence of a side reaction can also explain the increase of bulk resistance, since the use of TFSI anions in a side reaction decreases the salt concentration. This was also supported by the fact that the decrease of salt concentration is indicated in the ex situ PGStE-NMR study. On the other hand, a homogeneous Cl distribution is seen in Figure 8e, so that the ClO_4^- ions are not involved in a side reaction. In fact, we obtained better cycle performance using LiClO_4 salts instead of LiTFSI in an SPE film.^[10,23] Hence, the development and optimization of Li salts would be beneficial to the improvement of the cycle performance of LPBs.

3. Conclusions

Using AC impedance techniques, ex situ PGStE-NMR methods, and ex situ SEM/EDS observations, we analyzed the capacity fading mechanism that appears in LPBs that contain plasticizers. LPBs that contain B-PEG and Al-PEG plasticizers showed an abrupt capacity decrease after tens of stable cycles. This decrease of capacity retention is related to an undesirable side reaction that occurs at the SPE|cathode interface, which may be caused by the decomposition of anions. The use of Li salts in this side reaction would also decrease the salt concentration in the bulk of the SPE, followed by an increase of the bulk resistance. Accordingly, the selection of Li salts would be one of the crucial factors in designing long-lifetime LPBs.

4. Experimental

Preparation of SPE Film: The plasticizers of B-PEG and Al-PEG were synthesized by the reaction of methoxy poly(ethylene glycol) $\text{CH}_3\text{O}(\text{CH}_2\text{CH}_2\text{O})_9\text{H}$ and B or Al containing compounds, boric acid anhydride (B_2O_3) or aluminum isopropoxide (Fig. 9). The starting mixtures with a stoichiometric ratio were dissolved in toluene under an inert gas atmosphere and refluxed at 100°C to eliminate water or isopropyl alcohol generated by the reaction. Since the obtained B-PEG and Al-PEG were sensitive to hydrolysis, the compounds were handled under water-free conditions, such as in an Ar-filled glove box. The details of the preparation are described in the literature [5,9].

The matrix for the polymer electrolytes was a copolymer of two types of poly(ethylene glycol) methacrylate (PEGMA): PEG-monomethacrylate (abbreviated to PME400, Nippon Nyukazai Co. Ltd) and PEG-dimethacrylate (PDE600, NOF Co. Ltd), as shown in Figure 10. Two kinds of plasticizers, B-PEG or Al-PEG were added in equal amounts to the matrix polymer in weight. LiTFSI (Fluka), was dissolved in the above solution to give a molar ratio of lithium and ethylene oxide (EO) units in polymer electrolyte of 1/20. Benzophenone was also added into the matrix polymer solution as an initiator for polymerization (0.5 wt % of matrix polymer). The above prepared mixtures were cast onto a poly(ethylene terephthalate) (PET) film by a doctor blade method. The mixtures were polymerized by UV radiation for an hour and heated for overnight at around 80°C to complete the polymerization reaction. Self-standing SPE films of approximately $100\ \mu\text{m}$ thickness were obtained. All the film preparation

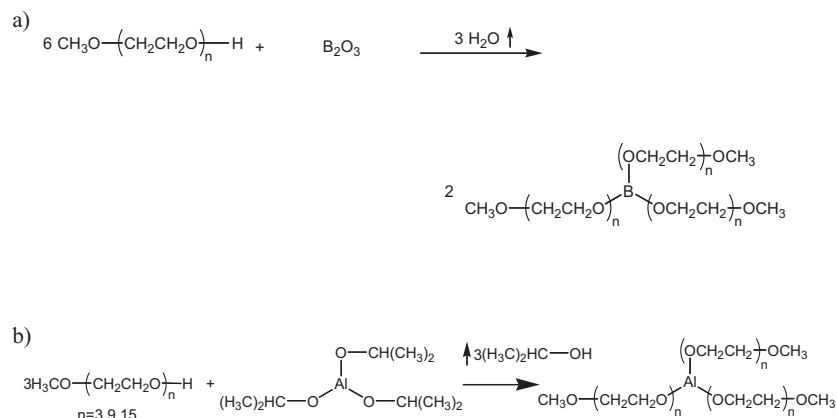


Figure 9. Scheme of the reaction for a) B-PEG and b) Al-PEG.

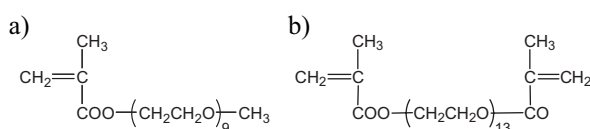


Figure 10. Molecular structures of poly(ethylene glycol)methacrylates: a) poly(ethylene glycol) (400) monomethacrylate (PME400), b) poly(ethylene glycol) (600) dimethacrylate (PDE600).

procedures were performed in an Ar-filled glovebox to ensure water-free conditions.

Preparation of the Cathode Sheet, LPB Fabrication, and Electrochemical Tests: A cathode active material of LiFePO₄ (Aldrich) with an olivine-type structure [24] were used in this study, since the operation voltage did not reach oxidation limit of the SPE film (~4.2 V) [5–9]. The cathode sheet consisted of 80 wt % active material, 5 wt % acetylene black as an electronic conductive agent, and a PEO–LiClO₄ complex as a lithium ion conductor and binder (molecular weight of PEO was ~1 000 000). These materials were mixed and dissolved in acetonitrile (AN) and cast onto aluminum sheets, the solvent was evaporated in a vacuum oven, and the product was then pressed into sheets. The obtained cathode sheet, SPE film, and lithium foil were cut into disks, and they were stacked inside a coin-type cell. Details of the preparation of the cathode sheets are presented in Ref. [11]. Charge–discharge tests for the prepared LPBs were performed galvanostatically at cut-off voltages of 3.0–3.8 V for LiFePO₄ cathode materials, respectively, at an operation temperature of 60 °C and a current density of 1.0 C (~200 μm). Before electrochemical measurement, the assembled coin cell was aged in the thermostat at the cell operation temperature (60 °C) for 24 h to enhance the adhesion of Li|SPE|cathode interfaces, unless specially mentioned. The AC impedance measurements were performed for a coin-type cell with Li|SPE|cathode construction using a VMP3 multichannel potentiostat equipped with impedance modules (Biologic). The frequency range was set from 10^{−2} to 10⁵ Hz. Note that LPB fabrications and electrochemical performance evaluations were repeated at least five times per sample to confirm the reproducibility of the electrochemical performance. The electrochemical data given in this paper is the best obtained, but the differences are small enough not to affect the discussion presented, unless specially mentioned.

Ion Transport Study Using PGStE-NMR and Impedance Techniques: SPE films were prepared by the same method mentioned in the above. The thickness of the SPE film was controlled to be larger than 1 mm in order to accurately evaluate the ion transport properties by PGStE-NMR and AC impedance methods. SPE films using B-PEG plasticizer before and after charge–discharging samples were used for the measurements. For the preparation of the latter sample, LPBs were constructed using SPE films with B-PEG plasticizer and cycled 50 times under a current density of 0.5 C

(~100 μm). The SPE films were then removed from the cell and placed in an Ar-sealed glass tube for PGStE-NMR measurement. Note that all the operations for SPE film preparation were performed in an Ar-filled glove box.

The ⁷Li and ¹⁹F NMR experiments were carried out by means of a Bruker Avance DSX 300 NMR spectrometer operating at 300.11 MHz for ¹H with a field-gradient generator system (with the maximum field-gradient strength: 11.60 T m^{−1}). The PGStE method that consisted of a π/2 pulse–τ₁–π/2 pulse–τ₂–π/2 pulse–τ₁–echo sequence was employed for diffusion coefficient measurements as reported previously [17, 19, 25–27].

For the PGStE ⁷Li and ¹⁹F NMR measurements, a typical experiment is as follows. The echo signal intensity was measured by changing the gradient strength *G* from 1.5 to 11 T m^{−1}, and the gradient pulse interval Δ was 100–200 ms, and the two gradient pulse widths δ are 2.5 ms in the two τ₁ periods, which are 3.5 ms, and the recycle delay is 5 or 8 s. The temperature was set at 60 and 70 °C to reproduce the operating temperature of the LPB.

The temperature dependence of the ionic conductivity for the sample before cycling was determined by the AC impedance method using a Hewlett–Packard 4192 A LF impedance analyzer over the frequency range from 5 Hz to 13 MHz. The samples of SPE films of 1 mm thickness were sandwiched between two stainless steel electrodes in the Ar-filled air tight vessel. The experimental details are described elsewhere [11].

Acknowledgements

The authors thank the Industrial Technology Research Grand Program from the New Energy and Industrial Technology Development Organization (NEDO) of Japan (Project ID: 06A23003c) for financial aid. SEM/EDS images for Figure 8 were taken by the Center for Advanced Materials Analysis (CAMA), Tokyo Institute of Technology, Japan. The authors' appreciation is extended to Mr. Y. Masuda, Tokyo Institute of Technology, for his precious advice and constructive suggestions. The B-PEG plasticizer was kindly supplied by NOF corporation, Japan. The Al-PEG plasticizer was kindly supplied by Nippon-Nyukazai Co., LTD, Japan.

Received: June 11, 2008

Revised: October 6, 2008

Published online: February 18, 2009

- [1] M. B. Armand, J. M. Chabagno, M. J. Duclot, in *Fast Ion Transport in Solids* (Eds: P. Vashista, J. N. Mundy, G. K. Shenoy), North Holland, Amsterdam **1979**.
- [2] A. S. Aricó, P. G. Bruce, B. Scrosati, J.-M. Tarascon, W. van Schalkwijk, *Nat. Mater.* **2005**, *4*, 366.
- [3] a) D. E. Fenton, J. M. Parker, P. V. Wright, *Polymer* **1973**, *14*, 589; b) P. V. Wright, *Br. Polym. J.* **1975**, *7*, 319.
- [4] P. P. Prosini, T. Fujieda, S. Passerini, M. Shikano, T. Sakai, *Electrochem. Commun.* **2000**, *2*, 44.
- [5] Y. Kato, S. Yokoyama, H. Ikuta, Y. Uchimoto, M. Wakihara, *Electrochem. Commun.* **2001**, *3*, 128.
- [6] Y. Kato, K. Hasumi, S. Yokoyama, T. Yabe, H. Ikuta, Y. Uchimoto, M. Wakihara, *Solid State Ionics* **2002**, *150*, 355.
- [7] Y. Kato, K. Suwa, S. Yokoyama, T. Yabe, H. Ikuta, Y. Uchimoto, M. Wakihara, *Solid State Ionics* **2002**, *152*, 155.
- [8] Y. Kato, S. Yokoyama, T. Yabe, H. Ikuta, Y. Uchimoto, M. Wakihara, *Electrochim. Acta* **2004**, *50*, 281.
- [9] Y. Masuda, M. Seki, M. Nakayama, M. Wakihara, H. Mita, *Solid State Ionics*, **2006**, *177*, 843.

- [10] a) F. Kaneko, Y. Masuda, M. Nakayama, M. Wakihara, *Cyclic Performances of All Solid-State Lithium Polymer Batteries Containing 13 Group Alboxide as Plasticizer*, presented at the 16th International Conference on Solid State Ionics, Shanghai, China **2007**; b) F. Kaneko, *Fabrication and Characterization of All-Solid-State Lithium Polymer Battery*, Masters Thesis, Tokyo Institute of Technology Japan **2008**.
- [11] Y. Masuda, M. Nakayama, M. Wakihara, *Solid State Ionics* **2007**, 178, 981.
- [12] A. Yamada, H. Koizumi, S. Nishimura, N. Sonoyama, R. Kanno, M. Yonemura, T. Nakamura, Y. Kobayashi, *Nat. Mater.* **2006**, 5, 357.
- [13] S. Seki, Y. Kobayashi, H. Miyashiro, Y. Mita, T. Iwahori, *Chem. Mater.* **2005**, 17, **2041**.
- [14] D. Aurbach, M. D. Levi, E. Levi, H. Teller, B. Markovsky, G. Salitra, *J. Electrochem. Soc.* **1998**, 145, 3024.
- [15] D. Aurbach, K. Gamolsky, B. Markovsky, G. Salitra, Y. Gofer, U. Heider, R. Oesten, M. Schmidat, *J. Electrochem. Soc.* **2000**, 147, 1322.
- [16] D. Ostrovskii, F. Ronci, B. Scrosati, P. Jacobsson, *J. Power Sources* **2001**, 94, 183.
- [17] E. L. Hahn, *Phys. Rev.* **1950**, 80, 580.
- [18] See such as, A. J. Bard, L. R. Faulkner, in *Electrochemical Methods, Fundamentals and Applications*, John Wiley & Sons, New York **2001**.
- [19] O. E. Stejskal, E. J. Tanner, *J. Chem. Phys.* **1965**, 42, 288.
- [20] S. Tabata, T. Hirakimoto, M. Nishiura, M. Watanabe, *Electrochim. Acta* **2003**, 48, 2105.
- [21] H. Shobukawa, H. Tokuda, S. Tabata, M. Watanabe, *Electrochim. Acta* **2004**, 50, 305.
- [22] G. G. Amatucci, C. N. Schmutz, A. Blyr, C. Sigala, A. S. Gozdz, D. Larcher, J. M. Tarascon, *J. Power Sources* **1997**, 69, 11.
- [23] Y. Masuda, *Masters Thesis*, Tokyo Institute of Technology (Japan) **2007**.
- [24] A. K. Padhi, K. S. Nanjundaswamy, J. B. Goodenough, *J. Electrochem. Soc.* **1997**, 144, 1188.
- [25] S. W. Price, *Annu. Rep. NMR Spectrosc.* **1996**, 32, 51.
- [26] P. T. Callaghan, in *Principles of Nuclear Magnetic Resonance Microscopy*, Clarendon Press, Oxford **1991**.
- [27] R. Kimmich, in *NMR: Tomography, Diffusiometry, Relaxometry*, Springer, Berlin **1997**.